Journal of Sound and Vibration (1997) **208**(1), 15–32

ACTIVE CONTROL OF FORCED AND UNFORCED STRUCTURAL VIBRATION

P. Salemi and M. F. Golnaraghi

Mechanical Engineering Department, University of Waterloo, Waterloo, Ontario N2L 3G1, Canada

AND

G. R. Heppler

Systems Design Engineering Department, University of Waterloo, Waterloo, Ontario N2L 3G1, Canada

(*Received* 20 *May* 1996, *and in final form* 19 *May* 1997)

An analytical approach to vibration control is presented, and verified experimentally, for cases where it is undesirable to add actuators with significant mass and stiffness to the structure. A linear coupling control (LCC) strategy is implemented by coupling a second order linear system to an oscillatory plant to create an energy exchange between the two component systems. One of the advantages of this approach is that the control strategy is ultimately capable of controlling unforced and periodically forced vibrations in the plant.

The paper covers the application of the LCC control strategy to a cantilevered beam actuated by piezoceramic actuators. A novel model for the piezoactuated beam is derived for any representative mode, resulting in a set of linearized equations. Also, the model provides flexibility in actuator location and dimensions.

The controller is modelled as a single-degree-of-freedom linear oscillator which is coupled to the plant via linear terms. The result is a small actuating force, or weak coupling between plant and controller which lends itself well to piezoceramic actuation. This system is solved as a linear eigenvalue problem which provides a computationally efficient means of finding the response.

The solution is also verified by means of a finite element (FE) simulation which is carried out for both free and forced vibration. Apart from confirming the theoretical model and closed-form solution, the FE method provides another flexible means in predicting the response of the LCC strategy, the control strategy and the theoretical studies have been verified experimentally.

1. INTRODUCTION

The notion of using secondary coupled systems for vibration absorption is well established both analytically and in practice [1, 2]. In many contemporary engineering works traditional control methods cannot be used either because the required actuators are too heavy for the application at hand or because the method itself cannot cope with the circumstances of the application. Applications of this sort include space structures such as satellites, or other structures that must be considered as flexible in an analysis of their dynamic behaviour. In the case of a space structure there is typically very low inherent damping in the structure so that there will most likely be significant residual oscillations from slewing motions. In the case of robots the decreased stiffness results in a loss of accuracy in terms of end effector positioning.

0022–460X/97/460015 + 18 $25.00/0/sv971142

This paper examines the control of structural vibration by means of an energy based strategy that exploits the beat phenomenon. This is a phenomenon which may be observed in two coupled linear systems that have frequencies tuned very close to each other. The result is a fast oscillation in each system modulated by a slow envelope frequency. Control is accomplished by coupling the plant and the controller in such a manner that an exchange of energy between the two is achieved. A significant feature of this strategy is that the same controller may also be used to quell forced excitation, in addition to free vibration.

The notion of using an energy based controller was originally exploited by Golnaraghi [3]. This work established a non-linear coupling characteristic, defined as Internal Resonance (IR), because a clamped–free flexible beam and a spring-mass-slider. Subsequently, the slider mechanism was replaced by a motor with a rotating moment arm, Khajepour *et al*. [4]. The equations for this system are dynamically coupled and contain quadratic non-linearities, which were exploited for control purposes. The system was realized experimentally later on and it was found that the first mode of the primary beam could be controlled for a variety of initial conditions.

Tuer *et al*. [5, 6] have shown that linear co-ordinate coupling can be used as an energy exchange technique and unlike the nonlinear coupling control of Golnaraghi [3], which exploited modal interactions, the linear controller exploits coupling between co-ordinates. It was shown that the maximum transfer of energy was obtained when the natural frequencies of the plant and the controller were equal. Furthermore, the linearly coupled system considered in these previous efforts, and in this paper are shown to be stable for all practical purposes. The stability analysis using the eigenvalue problem model and the Lyapunov method has fully been addressed in Khajepour *et al*. [4] for a general class of linear coupled controllers, and hence, is not mentioned here.

Also, under certain system parameters all the plant energy could be extracted by the first local minimum in the output signal. Similarly, works by Morris and Juang [7] and Juang and Phan [8] use a linearly coupled system as a dissipative controller. The approach in these works is similar in that a coupled linear system is employed. However, the fundamental difference is that the LCC strategy relies on the beat phenomenon and decoupling at a minimum, and not active/passive energy dissipation.

Oueini and Golnaraghi [9] was able to replace the secondary systems used by Golnaraghi [3], Tuer *et al*. [5, 6] with an internal resonance that was built as a coupled oscillator implemented in analog circuitry that emulates the equation of the controller.

The work presented in this paper continues from these previous works in coupling control, by examining the possibility of controlling the free and forced (periodic forcing) vibration of a beam using piezoceramic actuators. The approach of using piezoceramics for control has been established by Crawley and Anderson [10], and furthered by others such as Inman *et al*. [11]. However, in this work piezoceramics are incorporated as part of the LCC strategy, which amounts to replacing a physical vibration absorber with an electromechanical (piezoelectric and circuit) counterpart. The most notable distinction of this controller from classical state feedback controllers is that the same coupling controller is used to control both the free and the forced case.

The configuration for the present beam is a clamped–free flexible beam with the vibration occurring in a plane that is parallel to the ground. This orientation was selected so that the effects of gravity could be ignored in the modelling. The actuators are piezoceramic elements rigidly bonded to a portion of the beam. Analytical models for an actuator/beam system have been examined in the past by Patnaik *et al*. [12, 13]. This paper incorporates the properties of the actuator into that of the substructure. Thus, modelling for the system is carried out by partitioning the domain into actuated and non-actuated regions and deriving the equations of motion for the whole by applying appropriate

continuity conditions. The result is a model which may have ultimately been used for placing piezoceramics anywhere along the length of the beam. Moreover, the model provides the flexibility to analyze any number of modes of vibration, however for this work multi-mode vibration control is left to further examination in subsequent work by researchers in the same university research group. The beam equations are coupled with a single-degree-of-freedom, linear, second order differential equation, which models a linear oscillator physically coupled to the plant.

The plant and controller governing equations are considered analytically with the intention of finding a closed form solution, and an approach to solving these equations is detailed. The result is a computationally efficient solution for the response of the beam/controller system.

The same system configuration is also analyzed with the finite element method, in order to verify the developed model and provide another flexible means of solving the response. The FE matrices are augmented to include the extra degree of freedom assigned to the controller. Both the free vibration and forced vibration scenarios are simulated, and the possibility of simulating different actuator configurations and dimensions is incorporated. In order to validate the theoretical and finite element results an experiment has been devised which is briefly described in this paper.

2. THEORETICAL FORMULATION OF SYSTEM

The development of the plant and controller models is illustrated for a cantilevered beam with piezoceramic actuators and the LCC controller. The beam is assumed to be separated into two regions; one region which has actuators attached to the beam and another region consisting of only the beam. Under the assumptions of the Euler–Bernoulli beam model expressions for the mode shapes and the frequency equation are derived. It must be noted that the partitioning in two regions has been used here only for convenience. In general, the actuators may be applied to an arbitrary location and a similar method may be used. Thereafter, the controller is described and the method of coupling is explained. Various expressions for describing the behaviour of the system are obtained from the plant and controller coupled system.

2.1. THE ACTUATED BEAM MODEL

A cantilevered beam with piezoceramic layers bonded to the substructure at the fixed end of the beam will be considered as shown in Figure 1.

Consistent with the assumptions for an Euler–Bernoulli beam it is assumed that axial loads and rotary inertia are negligible, and that plane sections remain plane and normal. It is also assumed that each region behaves according to the Euler–

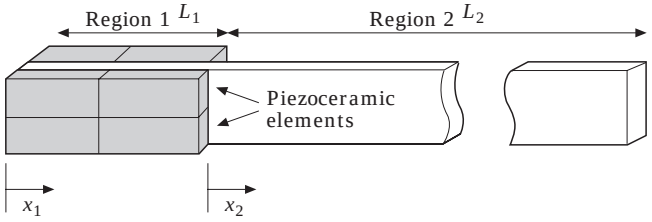

Figure 1. Cantilevered flexible beam model.

Bernoulli model and hence may be described by the beam equations governing that model. Hence,

$$E_1 I_1 y_1^{iv} + \rho_1 A_1 \ddot{y}_1 = 0, \quad 0 \leqslant x_1 \leqslant L_1, \qquad E_2 I_2 y_2^{iv} + \rho_2 A_2 \ddot{y}_2 = 0, \quad L_1 \leqslant x_2 \leqslant L_2, \quad \text{(1a, b)}$$

where $E_i I_i$ is the flexural rigidity of the ith region, $\rho_i A_i$ is the linear mass density of the region, and $i = \{1, 2\}$. The transverse displacement over the region i denoted by $y_i (x_i, t)$. To solve these equations, assume that y is separable in space and time, such that

$$y_1 (x_1, t) = \Phi_1 (x_1) Y_1 (t), \quad 0 \leqslant x_1 \leqslant L_1, \qquad y_2 (x_2, t) = \Phi_2 (x_2) Y_2 (t), \quad L_1 \leqslant x_2 \leqslant L_2. \tag{2a, b}$$

These may be substituted into equations (1) to yield

$$E_1 I_1 \Phi_1^{iv} Y_1 + \rho_1 A_1 \Phi_1 \ddot{Y}_1 = 0, \qquad 0 \leqslant x_1 \leqslant L_1, \tag{3a}$$

$$E_2 I_2 \Phi_2^{iv} Y_2 + \rho_2 A_2 \Phi_2 \ddot{Y}_2 = 0, \qquad L_1 \leqslant x_2 \leqslant L_2. \tag{3b}$$

Dividing through by Φ_i and $\rho_i A_i Y_i$, setting $\alpha_i = E_i I_i / (\rho_i A_i)$, and equating the result to the separation constant ω^2 yields separate equations in time and space expressed in symmetrical form by:

$$\alpha_1 \frac{\Phi_1^{iv}}{\Phi_1} = -\frac{\ddot{Y}_1}{Y_1} = \omega^2, \quad 0 \leqslant x_1 \leqslant L_1 ; \qquad \alpha_2 \frac{\Phi_2^{iv}}{\Phi_2} = -\frac{\ddot{Y}_2}{Y_2} = \omega^2, \quad L_1 \leqslant x_2 \leqslant L_2. \tag{4b}$$

The spatial equations are readily shown to lead to an eigenvalue problem which may be formulated as follows:

$$\alpha_1 \Phi_1^{iv} - \omega^2 \Phi_1 = 0, \quad 0 \leqslant x_1 \leqslant L_1 ; \qquad \alpha_2 \Phi_2^{iv} - \omega^2 \Phi_2 = 0, \quad L_1 \leqslant x_2 \leqslant L_2. \tag{5a, b}$$

Equations (5) have a characteristic equation of the form

$$s^4 - \beta_i^4 = 0 \tag{6}$$

so that the characteristic roots are $s_{1,2} = \pm \beta_i$ and $s_{3,4} = \pm \mathrm{j} \beta_i$ where $\beta_i^4 = \omega^2 \alpha_i$ and $\mathrm{j} = \sqrt{-1}$. Consequently, the general solutions to (5) are

$$\Phi_1 (x_1) = A_1 \cos (\beta_1 x_1) + A_2 \sin (\beta_1 x_1) + A_3 \sinh (\beta_1 x_1) + A_4 \cosh (\beta_1 x_1), \qquad 0 \leqslant x_1 \leqslant L_1, \tag{7a}$$

$$\Phi_2 (x_2) = B_1 \cos (\beta_2 x_2) + B_2 \sin (\beta_2 x_2) + B_3 \sinh (\beta_2 x_2) + B_4 \cosh (\beta_2 x_2), \qquad 0 \leqslant x_2 \leqslant L_2. \tag{7b}$$

Note here the assumption that there exists distinct eigenvalues β_i for each segment; however, each is a function of ω, which is the natural frequency for the whole beam. Boundary conditions for the clamped–free beam may be expressed as

$$\Phi_1 (0) = 0, \qquad \Phi_1' (0) = 0, \qquad \Phi_2'' (L_2) = 0, \qquad \Phi_2''' (L_2) = 0. \tag{8}$$

In addition it is required that there be continuity of displacement, rotation, moment, and shear at the boundary between the two segments of the beam so that

$$\Phi_1 (L_1) = \Phi_2 (0), \qquad \Phi_1' (L_1) = \Phi_2' (0), \qquad \Phi_1'' (L_1) = \Phi_2'' (0), \qquad \Phi_1''' (L_1) = \Phi_2''' (0). \tag{9}$$

Introducing the transformation $x_2 = x_1 - L_1$ allows each portion of equations (7) to be expressed in the same co-ordinate x_1 (which will be henceforth referred to as x). Thus, equations (7) may be written as

$$\Phi_1 (x) = A_1 \cos (\beta_1 x) + A_2 \sin (\beta_1 x) + A_3 \sinh (\beta_1 x) + A_4 \cosh (\beta_1 x), \qquad 0 \leqslant x \leqslant L_1, \tag{10a}$$

$$\Phi_2(x-L_1) = B_1\cos(\beta_2(x-L_1)) + B_2\sin(\beta_2(x-L_1)) + B_3\sinh(\beta_2(x-L_1)) + B_4\cosh(\beta_2(x-L_1)), \qquad L_1 \leqslant x \leqslant L_2, \quad (10b)$$

and the boundary conditions (8) must be re-expressed given the new reference frame, to yield

$$\Phi_1(0) = 0, \qquad \Phi_1'(0) = 0, \qquad \Phi_2''(L_1+L_2) = 0, \qquad \Phi_2'''(L_1+L_2) = 0, \quad (11)$$

while the continuity conditions (9) must be re-expressed to yield

$$\Phi_1(L_1) = \Phi_2(L_1), \qquad \Phi_1'(L_1) = \Phi_2'(L_1), \qquad \Phi_1''(L_1) = \Phi_2''(L_1), \qquad \Phi_1'''(L_1) = \Phi_2'''(L_1). \quad (12)$$

Substituting general solutions (10) into the boundary conditions (11) and the continuity conditions (12) results in a set of eight equations expressed in terms of the eight constants $A_1, \ldots, A_4, B_1, \ldots, B_4$. These equations may be expressed in matrix form, where a column vector contains the solution constants and the matrix contains transcendental expressions which are constant coefficients [14]. The matrix, defined as $\mathbf{E}$, is partitioned in order to simplify the evaluation of mode shape constants, and appears as

$$\mathbf{E} = \left[\begin{array}{c|c} \mathbf{E}_{11} & \mathbf{E}_{12} \\ (7\times 7) & (7\times 1) \\ \hline \mathbf{E}_{21} & E_{22} \\ (1\times 7) & \end{array}\right] \quad \left\{\begin{array}{c} \hat{\mathbf{A}}_1 \\ B_4 \end{array}\right\} = 0 \quad (13)$$

The element E_{22} is the coefficient of B_4 for boundary condition (11d) and $\hat{\mathbf{A}}_1$ represents the vector of constants A_1 to B_3 without element B_4. Consider

$$\mathbf{E}_{11}\,\hat{\mathbf{A}}_1 + \mathbf{E}_{12}\,B_4 = \mathbf{0}, \quad (14)$$

which may be rewritten and inverted to yield

$$\hat{\mathbf{A}}_1 = [-\mathbf{E}_{11}^{-1}\mathbf{E}_{12}]\{B_4\}. \quad (15)$$

The constant terms $\hat{\mathbf{A}}_1$ thus found are used in equation (10) to find the mode shapes for the beam. Furthermore, for a non-trivial solution the determinant of matrix $\mathbf{E}$ must equal zero, yielding a characteristic equation in β_i. Recall that $\beta_i^4 = \omega^2\alpha_i$, where ω is the natural frequency for the entire beam. The resulting characteristic equation is very long and complicated [14].

Now the governing equations (1) may be solved by assuming a series solution of the form:

$$y_1(x,t) = \sum_{r=1}^{n} \Phi_{r1}(x)\,Y_1(t), \qquad 0 \leqslant x \leqslant L_1, \quad (16a)$$

$$y_2(x,t) = \sum_{r=1}^{n} \Phi_{r2}(x)\,Y_2(t), \qquad L_1 \leqslant x \leqslant L_2, \quad (16b)$$

where the infinite series is truncated at n modes and x is the co-ordinate with origin at the base of the beam and having the domain $x\in[0, L_1 + L_2]$. Substituting equation (16) into equations (1) and dropping the summation to consider only the rth mode results in

$$E_1 I_1 \Phi_{r1}^{iv} Y_1 + \rho_1 A_1 \Phi_{r1}\ddot{Y}_1 = 0, \qquad 0 \leqslant x \leqslant L_1, \quad (17a)$$

$$E_2 I_2 \Phi_{r2}^{iv} Y_2 + \rho_2 A_2 \Phi_{r2} \ddot{Y}_2 = 0, \qquad L_1 \leqslant x \leqslant L_2. \tag{17b}$$

After taking the inner product of equation (17) with respect to Φ_{s1} and Φ_{s2}, integrating by parts twice, and making use of the boundary conditions (11) yields

$$E_1 I_1 ([\Phi_{s1} \Phi_{r1}''' - \Phi_{r1} \Phi_{s1}''']_{L_1} - [\Phi_{s1}' \Phi_{r1}'' - \Phi_{r1}' \Phi_{s1}'']_{L_1}) + \rho_1 A_1 (\omega_r^2 - \omega_s^2) \int_0^{L_1} \Phi_{r1} \Phi_{s1} \, \mathrm{d}x = 0 \tag{18}$$

and

$$E_2 I_2 ([\Phi_{s2} \Phi_{r2}''' - \Phi_{r2} \Phi_{s2}''']_{L_1} - [\Phi_{s2}' \Phi_{r2}'' - \Phi_{r2}' \Phi_{s2}'']_{L_1}) + \rho_2 A_2 (\omega_r^2 - \omega_s^2) \int_{L_1}^{L_2} \Phi_{r2} \Phi_{s2} \, \mathrm{d}x = 0. \tag{19}$$

Adding equations (18) and (19) and enforcing Betti's Law [15], which in essence implies that the first terms in each of equations (18) and (19) sum to zero, resulting in the inertial orthogonality relation

$$\rho_1 A_1 \int_0^{L_1} \Phi_{s1} \Phi_{r1} \, \mathrm{d}x + \rho_2 A_2 \int_{L_1}^{L_2} \Phi_{s2} \Phi_{r2} \, \mathrm{d}x = 0, \qquad s \neq r. \tag{20}$$

Similarly, the elastic orthogonality relation is given by

$$E_1 I_1 \int_0^{L_1} \Phi_{s1}'' \Phi_{r1}'' \, \mathrm{d}x + E_2 I_2 \int_{L_1}^{L_2} \Phi_{s2}'' \Phi_{r2}'' \, \mathrm{d}x = 0, \qquad s \neq r. \tag{21}$$

Introducing an external forcing term $f_i(x, t)$ into equation (1) and assuming the series solutions (16) gives

$$E_1 I_1 \sum_{r=1}^{n} \Phi_{r1}^{iv} Y_{r1} + \rho_1 A_1 \sum_{r=1}^{n} \Phi_{r1} \ddot{Y}_{r1} = f_1(x, t), \tag{22a}$$

$$E_2 I_2 \sum_{r=1}^{n} \Phi_{r2}^{iv} Y_{r2} + \rho_2 A_2 \sum_{r=1}^{n} \Phi_{r2} \ddot{Y}_{r2} = f_2(x, t). \tag{22b}$$

Taking the inner product with respect to Φ_{s1} and Φ_{s2}, upon applying the orthogonality conditions, and integration by parts twice yields the final result:

$$E_1 I_1 \int_0^{L_1} \Phi_{s1}'' \Phi_{s1}'' \, Y_1 \, \mathrm{d}x + \rho_1 A_1 \int_0^{L_1} \Phi_{s1} \Phi_{s1} \, \ddot{Y}_1 \, \mathrm{d}x = \int_0^{L_1} \Phi_{s1} f_1(x, t) \, \mathrm{d}x, \tag{23a}$$

$$E_2 I_2 \int_{L_1}^{L_2} \Phi_{s2}'' \Phi_{s2}'' \, Y_2 \, \mathrm{d}x + \rho_2 A_2 \int_{L_1}^{L_2} \Phi_{s2} \Phi_{s2} \, \ddot{Y}_2 \, \mathrm{d}x = \int_{L_1}^{L_1} \Phi_{s2} f_2(x, t) \, \mathrm{d}x. \tag{23b}$$

The forcing term may now be addressed. Under the assumption of perfect bonding, actuators effectively produce a bending moment on the beam. In that case, the forcing terms in equation (23) may be treated as point moments acting at the edges of the piezoceramic elements which, here, are at the base of the beam and at the interface L_1.

Therefore, $f_i(x, t)$ is expressed as point moments, or doublets, acting at $x = 0$ and $x = L_1$. This may be written as

$$\int_0^{L_1} \Phi_{s1} f_1(x, t)\,\mathrm{d}x = \int_0^{L_1} \Phi_{s1}\,\Gamma(t)\,[\delta'(x) - \delta'(x - L_1)]\,\mathrm{d}x, \tag{24}$$

where $\Gamma(t)$ is the magnitude of the moment assumed to be applied at either end of the piezoceramic region, (i.e., segment **1**). An identity for the Dirac delta function states

$$\int_0^a f(x)\delta'(x - a)\,\mathrm{d}x = f'(a). \tag{25}$$

Therefore the right side of equation (23a) may be written as

$$\int_0^{L_1} \Phi_{s1} f_1(x, t)\,\mathrm{d}x = [\Phi'_{s1}(L_1) - \Phi'_{s1}(0)]\Gamma(t). \tag{26}$$

The effect of the piezoceramics is assumed to be only on equation (23a), thus the right side of equation (23b) is set equal to zero. Since the beam is continuous at L_1, the resulting equation may be written in a combined form:

$$E_1 I_1 \int_0^{L_1} \Phi''_{s1}\,\Phi''_{r1}\,Y_1\,\mathrm{d}x + \rho_1 A_1 \int_0^{L_1} \Phi_{s1}\,\Phi_{r1}\,\ddot{Y}_1\,\mathrm{d}x + E_2 I_2 \int_{L_1}^{L_2} \Phi''_{s2}\,\Phi''_{r2}\,Y_2\,\mathrm{d}x$$

$$+ \rho_2 A_2 \int_{L_1}^{L_2} \Phi_{s2}\,\Phi_{r2}\,\ddot{Y}_2\,\mathrm{d}x = \gamma_1\,\Gamma(t), \tag{27}$$

where $\gamma_1 = [\Phi'_{s1}(L_1) - \Phi'_{s1}(0)]$, γ_1 is a parametric gain term resulting from the modal contribution of the point moments and will be implemented physically as the gain of the electromechanical coupling coefficients, and $\Gamma(t)$ is a general time varying function which will ultimately be replaced by some control law. The next section deals with the development of the controller which will be implemented on the plant's governing equations.

The general plant equation (27) may now be completed. The quantities in the integrals may be solved exactly since the mode shapes Φ_{si} and Φ_{ri} are known, and may be factored apart from the Y_i terms which are functions of time alone, yielding the following constants:

$$K_1 = E_1 I_1 \int_0^{L_1} \Phi''_{s1}\,\Phi''_{r1}\,\mathrm{d}x, \qquad M_1 = \rho_1 A_1 \int_0^{L_1} \Phi_{s1}\,\Phi_{r1}\,\mathrm{d}x, \tag{28a, b}$$

$$K_2 = E_2 I_2 \int_{L_1}^{L_2} \Phi''_{s2}\,\Phi''_{r2}\,\mathrm{d}x, \qquad M_2 = \rho_2 A_2 \int_{L_1}^{L_2} \Phi_{s2}\,\Phi_{r2}\,\mathrm{d}x \tag{28c, d}$$

Furthermore, it is also observed that the separated temporal solution for Y_i in equations (4) will show that $Y_1 = Y_2$. Thus, the constant terms may be reduced further given that $K = K_1 + K_2$ and $M = M_1 + M_2$. The final governing equation appears as

$$\ddot{Y} + \omega_p^2 Y = \gamma_1\,\Gamma(t), \tag{29}$$

where $\omega_p^2 = K/M$. Using the dimensions and properties of an actual physical system developed by Salemi [14], the value $\omega_p^2 = 27{\cdot}4$ rad/s is subsequently used.

3. CONTROLLER MODELLING

As stated previously, the aim of this research is to exploit the notion of energy exchange between linearly coupled systems. Having established a model for the cantilever beam, the primary system, the goal is to develop the equations of a coupled secondary system. Since this system does not necessarily need to exist in the physical sense, there is no need to consider material, dimensional, or other such properties. However, the system must behave as a linear oscillator which may be forced by an external linear input, and it must yield an output that may be coupled with the plant.

3.1. DESCRIPTION OF CONTROLLER STRATEGY

The plant equations that are derived in the previous section may be adapted to include some form of control strategy via the input provided by the piezoceramic actuators. The forcing term on the right side of equation (27) is evidently a function of some moment with magnitude $\Gamma(t)$; however, $\Gamma(t)$ is still an arbitrary input as yet undefined. At this point, any general control strategy could potentially be assigned to dictate the input to the plant. For example, a state feedback control law could be assigned to the input such that $\Gamma(t)$ is proportional to a set of time dependent states as described by Salemi *et al.* [16]. Or, given some reference point to be maintained in the plant, an error term could be implemented in a PID controller yielding some $\Gamma(t)$ input to the plant.

3.2. FORMULATION OF CONTROL EQUATIONS

The primary requirement of the coupling control strategy demands that the secondary system must be a linear oscillator. Such a system, in general, would be satisfied by a linear second order ordinary differential equation of the form

$$\ddot{U} + 2\zeta_c \omega_c \dot{U} + \psi_c^2 U = \gamma G(y, \dot{y}, \ddot{y}, t), \tag{30}$$

where $U(t)$ is a time dependent generalized controller co-ordinate, ζ_c is the controller damping ratio, ω_c is the controller's natural frequency, and $G(y, \dot{y}, \ddot{y}, t)$ is a generalized forcing input which is a function of a single, or linear combination of plant states $\ddot{y}$, $\dot{y}$ or y and is proportional to parametric gain γ.

Recall from equation (16) that the solution $y(x, t)$ for the plant equation may be separable in time and space. It is assumed that only the first mode of vibration is being considered. Thus the outputs of the generalized plant co-ordinate have the form:

$$y_i(x, t) = \Phi_i(x) Y_i(t), \qquad \dot{y}_i(x, t) = \Phi_i(x) \dot{Y}_i(t), \qquad \ddot{y}_i(x, t) = \Phi_i(x) \ddot{Y}_i(t). \tag{31a–c}$$

For the purpose of this research G is considered to be a function of only one of these plant states. In any of the states in equations (31), the function $\Phi_i(x)$ may be considered constant as it is independent of time. Moreover, $\Phi_i(x)$ may also be considered as an expression for sensor position along the length of the beam, where x is the given location of the sensor. The location of the sensor will therefore be designated as L_s, and the amplitude of the modal co-ordinate at L_s will therefore be $\Phi_i(L_s)$. The right side of equation (30) may be re-expressed as

$$\gamma G(y, \dot{y}, \ddot{y}, t) = \gamma \Phi_i(L_s) G(Y_i, \dot{Y}_i, \ddot{Y}_i, t). \tag{32}$$

The controller may now be expressed strictly in terms of the separated temporal plant states, and the controller's own frequency, damping and generalized co-ordinates:

$$\ddot{U} + 2\zeta_c\,\omega_c\,\dot{U} + \omega_c^2 U = \gamma_2\,G(Y_i,\,\dot{Y}_i,\,\ddot{Y}_i,\,t), \tag{33}$$

where $\gamma_2 = \gamma\Phi_i\,(L_s)$.

The final consideration that must be given to the controller is defining the output states which will force the plant. The input $\Gamma(t)$ from equation (27) may now be designated by some state of the controller co-ordinate, generally expressed as

$$\gamma_1\,\Gamma(t) = \gamma_1\,F(U,\,\dot{U},\,\ddot{U},\,t), \tag{34}$$

where $\ddot{U}$, $\dot{U}$ or U are any of the controller states: acceleration, velocity, and position output. And γ_1 is a parametric gain representing the magnitude of the moment applied by the piezoceramics.

The model derivation may now be completed in the next section by consolidating the plant and controller formulation into a unified expression for the system's governing equations. The plant equation and the controller equation (33) may now be written to complete the system governing equations:

$$\ddot{Y} + \omega_p^2 Y = \gamma_1\,F(U,\,\dot{U},\,\ddot{U},\,t), \tag{35a}$$

$$\ddot{U} + 2\zeta_c\,\omega_c\,\dot{U} + \omega_c^2 U = \gamma_2\,G(Y_i,\,\dot{Y}_i,\,\ddot{Y}_i,\,t). \tag{35b}$$

4. THEORETICAL SOLUTION

The dimensions and properties of the laboratory version are found in Table 1; this same plant is investigated theoretically according to the following analysis.

The plant and controller equations are implemented with specifically determined coupling states via attempting methods suggested in references [4] through [8] and then implemented through an iterative technique of plant/controller state analysis:

$$F(U,\,\dot{U},\,\ddot{U},\,t) = \dot{U}, \qquad G(Y_i,\,\dot{Y}_i,\,\ddot{Y}_i,\,t) = Y. \tag{36a, b}$$

In other words, the plant is forced by controller velocity and the controller is forced by plant position. The controller equations now appear as

$$\ddot{Y} + \omega_p^2 Y = \gamma_1\,\dot{U}, \qquad \ddot{U} + 2\zeta_c\,\omega_c\,\dot{U} + \omega_c^2 U = \gamma_2\,Y. \tag{37a, b}$$

The parameters used for this solution were obained from the model outlined in Salemi [14].

4.1. THEORETICAL RESULTS

The following plots are obtained by applying a diagonalization technique, found in Perko [17], to the system of equations (37), which may be written in the form $\mathbf{Ax} = \dot{\mathbf{x}}$, with initial conditions $\mathbf{x}(0) = \mathbf{x}_0$. An invertible matrix of eigenvectors $\mathbf{P}$ is found, which satisfies

$$\mathbf{P}^{-1}\mathbf{AP} = \operatorname{diag}\begin{bmatrix} a_j & -b_j \\ b_j & a_j \end{bmatrix}, \tag{38}$$

TABLE 1

Beam material and dimensional properties

Property	Material	Density (kg/m^3)	Young's Modulus (Gpa)	Length (mm)	Width (mm)	Thickness (mm)
Value	Al T-6061	2710	70	457·2	25·4	0·8

and the solution for $\mathbf{x}(t)$ may be written as

$$\mathbf{x}(t) = \mathbf{P}\ \text{diag}\ e^{a_j t} \begin{bmatrix} \cos(b_j)t & -\sin(b_j)t \\ \sin(b_j)t & \cos(b_j)t \end{bmatrix} \mathbf{P}^{-1}\mathbf{x}_0. \tag{39}$$

The following plots consist of the time response for Y, the plant position for both controlled and uncontrolled cases, and $\dot{U}$, the controller velocity i.e., output. The parameters used for this solution were obtained from the model outlined in Salemi [14]. Parameters that are varied in the following analysis are controller damping, frequency, and initial conditions. The coupling gains are set as $\gamma_1 = 53{\cdot}3$ and $\gamma_2 = 11{\cdot}2$ [14].

4.2. UNCONTROLLED RESPONSE

The uncontrolled free vibration response of the plant is shown in Figure 2 and clearly illustrates the minimal inherent damping in the system.

4.2. CONTROLLER TUNING

The process of tuning the controller involves the manipulation of controller frequency, damping, and initial condition. The plant is observed while varying controller frequency; recall the plant natural frequency is $\omega_p = 27{\cdot}4$ rad/s. Tuning the controller frequency near that of the plant results in a beating phenomenon; $\omega_c = 23$ rad/s is selected as yielding a discernible beat. Controller damping is manipulated in order to improve the plant response in achieving a better first minimum; a damping factor of $\zeta_c = 0{\cdot}09$ is applied. Manipulation of the controller initial velocity $\dot{U}(0)$ is used to change the initial kinetic energy of the system. The controller initial position, $U(0)$, is set equal to zero. The controller initial condition applied is $\dot{U}(0) = 0{\cdot}03$. From the response shown in Figure 3 it is clear that the coupled system demonstrates beating between the plant and controller. Also, it is seen that the response characteristics may be manipulated by changing controller conditions. Lastly, since the problem is linear it may be shown that the response may be solved for the time to first minimum, and subsequently this decay time may used for control.

4.4. CONTROLLER DISABLE TIME

Finally, to implement a controller disable in the solution an ODE numerical solver is used in MATLAB for simulation of τ_d, the disable time. Note that the plant minimum

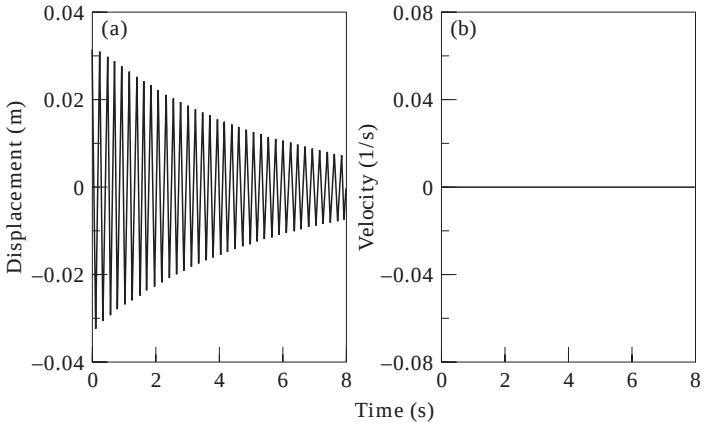

Figure 2. Uncontrolled response for free vibration: (a) plant response, (b) controller response.

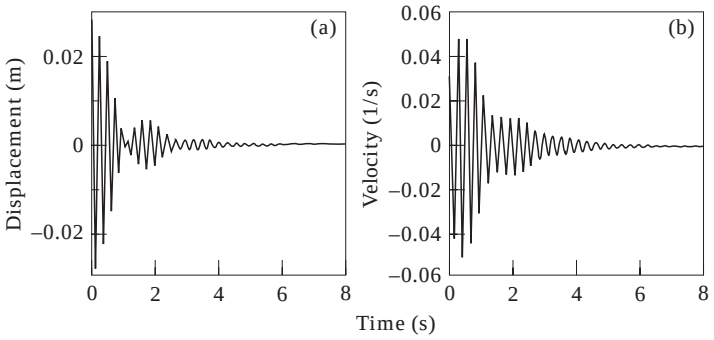

Figure 3. Plant and controller response from closed-form solution with $\omega_c = 23$ rad/s, $\zeta_c = 0{\cdot}09$, $\dot{U}(0) = 0{\cdot}03$: (a) plant response, (b) controller response.

in the previous case occurred after approximately 1 s, when solved numerically the controller is decoupled at 1·12 s, and thus the controller energy is not returned to the plant; see Figure 4.

The disable time for the controller is problem dependent only quantitatively. However, qualitatively, using the pseudo energy function,

$$E = \dot{x}^2/2 + \Omega^2 x^2/2, \tag{40}$$

where Ω is independently defined and hence may be used to trigger the disable time at an energy minimum, an examination of implementing this strategy is given in reference [4].

A finite element (FE) approach is selected to augment the closed form method that has been already outlined. Furthermore, the FE analysis better lends itself to the simulation of disabling the controller input at a plant minimum and the simulation of controlling external forcing.

5. FINITE ELEMENT

In order to extend the developed theoretical model to a more flexible simulation environment the governing equations establishd in the previous section are simulated by means of finite element analysis of the cantilever beam illustrated in Figure 1. This will allow the system to be analyzed for the disable–controller method and control of forced vibration, as discussed in the introduction. Modelling for the actuator forces may be

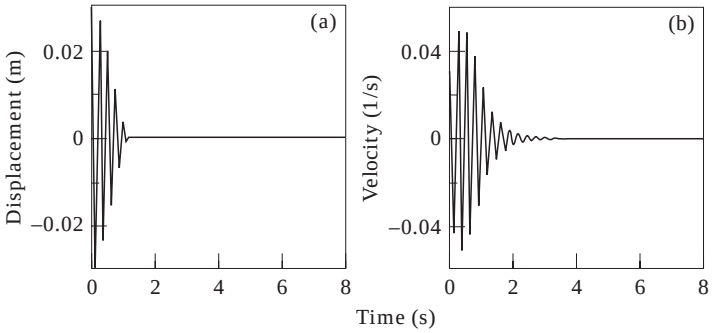

Figure 4. Plant and controller response from closed-form solution with $\omega_c = 23$ rad/s, $\zeta_c = 0{\cdot}09$, $\dot{U}(0) = 0{\cdot}03$, $\tau_d = 1{\cdot}12$ s: (a) plant response, (b) controller response.

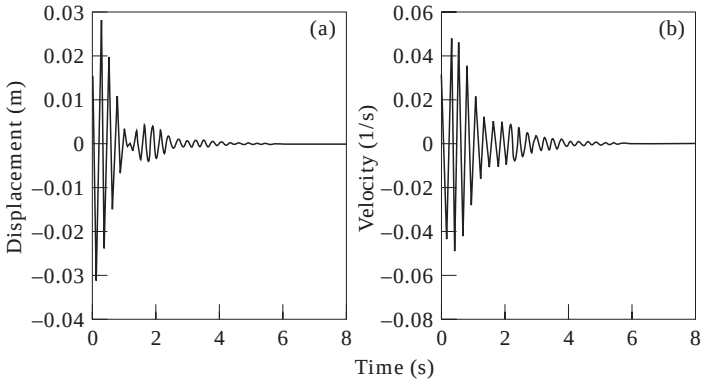

Figure 5. FE response $\omega_c = 23$ rad/s, $\zeta_c = 0{\cdot}09$, $\dot{U}(0) = 3$: (a) plant response, (b) controller response.

referred to in Patnaik [13] and the FE analysis may be referred to in Salemi [14]. The simulations are for a cantilever beam identical to that used in an experimental study to be described later in this paper. The final system of equations now appears in state space as follows:

$$\begin{pmatrix} 1 & 0 \\ 0 & 1 \end{pmatrix} \begin{pmatrix} \ddot{Y} \\ \ddot{U} \end{pmatrix} + \begin{pmatrix} 0 & -\gamma_1 \\ 0 & 2\zeta_c\,\omega_c \end{pmatrix} \begin{pmatrix} \dot{Y} \\ \dot{U} \end{pmatrix} + \begin{pmatrix} \omega_p^2 & 0 \\ -\gamma_2 & \omega_c^2 \end{pmatrix} \begin{pmatrix} Y \\ U \end{pmatrix} = \begin{pmatrix} \mathscr{F} \sin(\omega_{dr}\, t) \\ 0 \end{pmatrix}, \tag{41}$$

where an addition of an external steady state harmonic excitation of the form $\mathscr{F} \sin(\omega_{dr}\, t)$ is included. For the case of free vibration $\mathscr{F}$ is set equal to zero.

Therefore, what remains is the selection of controller frequency ω_c, controller damping ζ_c, controller initial condition $\dot{U}(0)$, and controller disable time τ_d. The coupling gains are set consistently with those in the theoretical formulation. The following subsections present results for the free and forced simulations.

5.1. FREE VIBRATION CONTROL SIMULATIONS

As in section 4 the parameter analysis for the control of free vibration examines the variation of parameters in the order mentioned above: ω_c, ζ_c, $\dot{U}(0)$, and τ_d. Using the parameter settings $\omega_c = 23$ rad/s, $\zeta_c = 0{\cdot}09$, and $\dot{U}(0) = 3$ the notion of a beat phenomenon between the plant and controller is reproduced in a FE simulation as shown in Figure 5. The controller initial condition $\dot{U}(0)$ has been re-scaled in the FE analysis by a factor of $\times 100$ [16].

5.1.1. *Controller disable time*

The disable time is introduced to the FE simulations by observing that severing the controller coupling leaves the plant with a specific position and velocity, or total energy. With the link to the controller removed, the energy in the plant is dissipated through internal damping. Of course the goal of this control strategy is to initiate the plant/controller decoupling at the optimal time: when it leaves a minimum energy level in the plant. This principle is illustrated in the simulations in Figure 6.

Note that if the controller is decoupled at any time prior or after the optimal disable time, the plant is left with remnant oscillations due to left over energy. However, the result for $\tau_d = 1{\cdot}12$ s, is timed perfectly such that remnant oscillations are virtually eliminated.

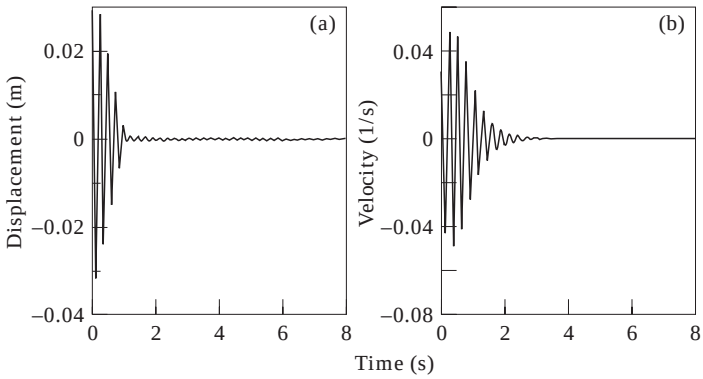

Figure 6. Plant and controller response from FE analysis with $\omega_c = 23$ rad/s, $\zeta_c = 0{\cdot}09$, $\dot{U}(0) = 3$, $\tau_d = 1{\cdot}12$ s: (a) plant response, (b) controller response.

5.2. COMPARISON OF THEORETICAL AND FE RESULTS

By manipulating the parameters of the controller in either method it is possible to affect the response of the plant. Each method indicates that a controller frequency that is tuned near the plant frequency will result in a beat phenomenon. Furthermore, each method shows that an energy minimum in the plant may be created such that the controller has extracted the plant vibration.

Also, the envelopes of the responses in the FE case show that the theoretical approach has a consistent result. This is valuable in preparation for experimental work, in that either model may be used to predict a laboratory methodology that could be used.

In summary, the process that is outlined and simulated using theoretical methods and finite elements yields clear evidence of the effectiveness of this strategy. The concept of vibration absorption as an active control method will be complete in the next section for control of forced vibration.

5.3. FORCED VIBRATION CONTROL SIMULATIONS

Although well known in its passive form, vibration absorption is enhanced by means of the LCC strategy which essentially amounts to an active vibration absorber. The advantage here lies in the flexibility of the application, which allows for variation in coupling and other parameters. The control of forced vibration involves significantly less parameter manipulation than in free vibration control. The controller frequency is chosen to be the same as in free vibration control because it affords the best energy exchange between co-ordinates, while maintaining stability. Furthermore, since forced control involves a steady-state output of the controller co-ordinate, the values of initial conditions $\dot{U}(0)$ and disable time τ_d are inconsequential. Hence what remains to be analyzed is the effect of controller damping on the plant response.

The forced input to the plant is modelled as a support excitation input $y = \mathscr{F} \cos(\omega_{dr} t)$ for which the system has a general governing equation of the form

$$\ddot{x} + 2\zeta_p \omega_p (\dot{x} - \dot{y}) + \omega_p^2 (x - y) = 0, \tag{42}$$

where ω_{dr} is the driving frequency of the excitation. The final form of this equation which is implemented in MATLAB code found in Salemi [16] is

$$\ddot{x} + 2\zeta_p \omega_p \dot{x} + \omega_p^2 x = \omega_p^2 \mathscr{F} \cos(\omega_{dr} t) - 2\zeta_p \omega_p \mathscr{F} \omega_{dr} \sin(\omega_{dr} t). \tag{43}$$

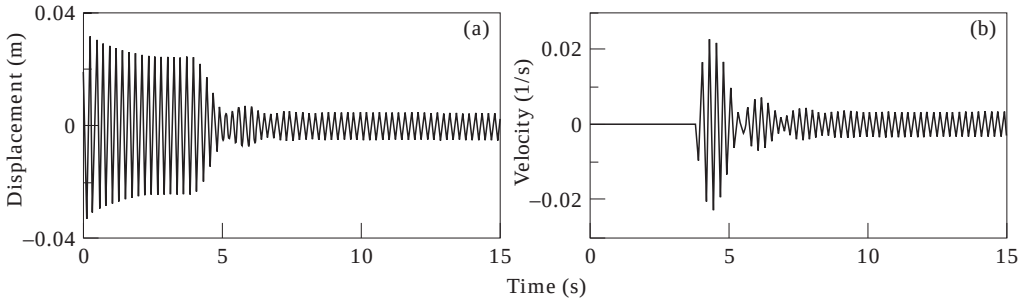

Figure 7. Forced vibration response from FE analysis $\zeta_c = 0{\cdot}09$: (a) plant response, (b) controller response.

The method applied to activating the controller involves simulating the uncontrolled response until transients have dissipated, and then turning on the controller by introducing the coupling terms, and continuing the simulation from the final states of the uncontrolled response.

5.3.1. *Controller damping*

The controller damping is implemented for a single case, and is illustrated in Figure 7 for $\zeta_c = 0{\cdot}09$. The simulation shows the controller activated at one quarter of the total simulation time. Percentage improvement over the uncontrolled response is calculated. This is defined as one minus the ratio of the controlled amplitude to the uncontrolled amplitude. This response is drastically improved by the control activation, the percentage improvement is 83·6%. This is more evident by comparing the FFT of the uncontrolled forced vibration versus the controlled forced vibration response shown in Figure 8.

6. EXPERIMENTS

In order to validate the theoretical and finite element results an experiment was devised, which is summarized as follows. The plant upon which the controller is implemented consists of a cantilevered beam such that the oscillations are planar. The base is clamped to a massive aluminum test bed such that the plant is sufficiently isolated from any extraneous vibration. The beam is made of aluminum sheet metal with material and dimensional properties as given in Table 1.

The actuators consist of two banks of four thin piezoceramic elements rigidly bonded to each side of the beam at the clamped end as shown in Figure 1. The length of the beam

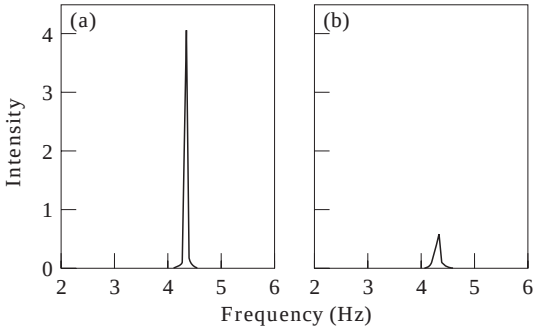

Figure 8. FFT for forced vibration: (a) uncontrolled response, (b) controlled response.

TABLE 2

Actuator material and dimensional properties

Property	Material	Density (kg/m^2)	Young's Modulus (Gpa)	Charge Constant d_{31} (C/m)	Length (mm)	Width (mm)	Thickness (mm)
Value	BM-532	7350	71·4	-200×10^{-12}	76·2	25·4	0·6

covered by the piezoceramic actuator is 75 mm. The actuator material is a PZT ceramic model BM532 produced by BM Hi-Tech Ltd. The actuator material properties and dimensions for a single element are given in Table 2. The elements are bonded with a BM Hi-Tech proprietary epoxy, and are arranged such that the dielectric poles of all elements are pointing in the same direction. When soldered, the positive lead is joined to all sides facing outward from the beam. The negative lead is bonded to the substructure, because the epoxy is sufficiently conductive to permit current to flow to the undersides of the elements facing the substructure. Hence, the same alternating signal can drive both banks of actuators at 180° out of phase. The deflection of the beam is measured using a strain gauge (Measurement Group Gauge, type EA-B-125TQ350) bonded as shown in Figure 1.

Strain gauges placed at the base of the beam provide a signal proportional to deflection, which is pre-amplified by a custom made circuit, and filtered by a commercial filter (Krohn-Hite 3322) set for low pass. The beam output is displayed on a Nicolet 310 digital oscilloscope. The conditioned signal is differentiated twice on a custom made board such that all plant states, position, velocity, and acceleration are known and may be used for controller coupling. The signal is fed to the controller and a feedback output is generated from the analog circuitry. The output of the controller is conditioned for amplification by a high voltage power supply (HVPS), and subsequently excites the piezoceramics.

For free vibration control, the beam is clamped such that a release mechanism can create different repeatable initial conditions. For forced vibration, the configuration shown in Figure 9 is mounted on a custom built harmonic oscillator.

The results for both the control of free and forced vibrations, shown in Figures 10 and 11, correspond well with the theoretical results.

The delay time constant τ_d is set by means of varying a potentiometer resistance. Selection of τ_d is made by means of previous test observations, whereby, upon noticing the minimum time on the previous plots it is possible to converge to the time by trial and

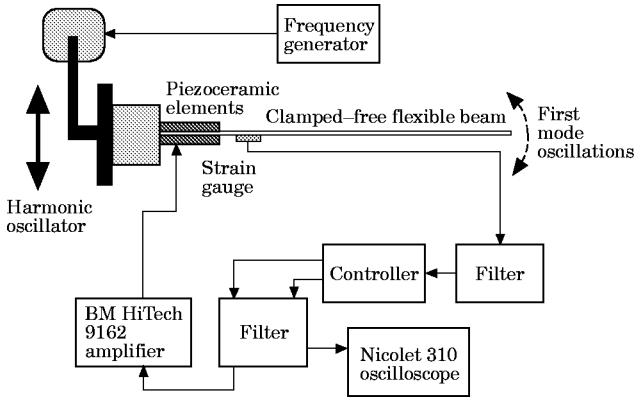

Figure 9. Schematic diagram of experimental apparatus.

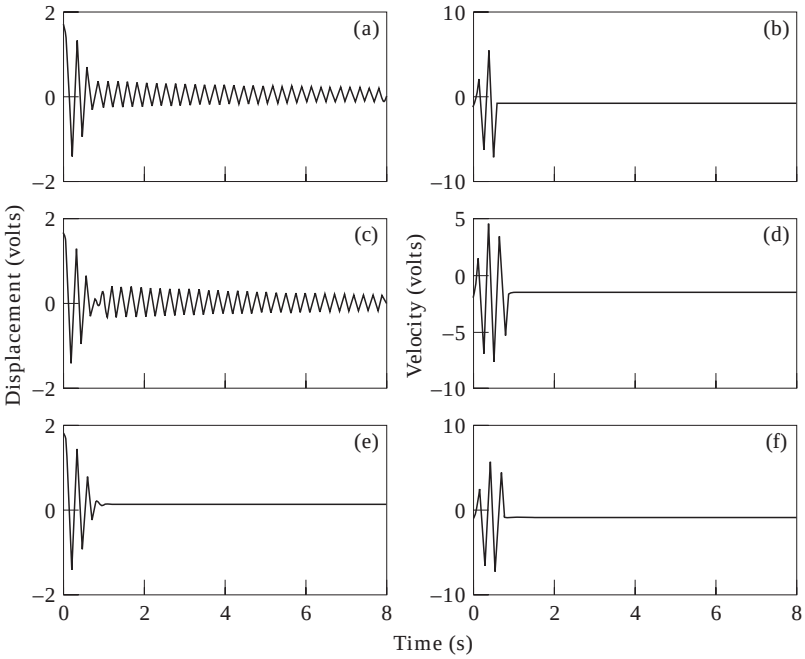

Figure 10. Experimental controlled free response; $\omega_c = 24$ rad/s, $\zeta_c = 0{\cdot}13$, $IC_c = 4{\cdot}5$; (a) $\tau_d = 0{\cdot}74$, (b) controller, (c) $\tau_d = 1{\cdot}31$, (d) controller, (e) $\tau_d = 0{\cdot}91$, (f) controller.

error. Figures 10(a), 10(c), and 10(e) show the responses for $\tau_d = 0{\cdot}74$, $\tau_d = 1{\cdot}31$ and $\tau_d = 0{\cdot}91$. Figures 10(b), 10(d), and 10(f) show the respective controller responses. The results in Figure 10 show that the delay is critical to the response. A disable time that is

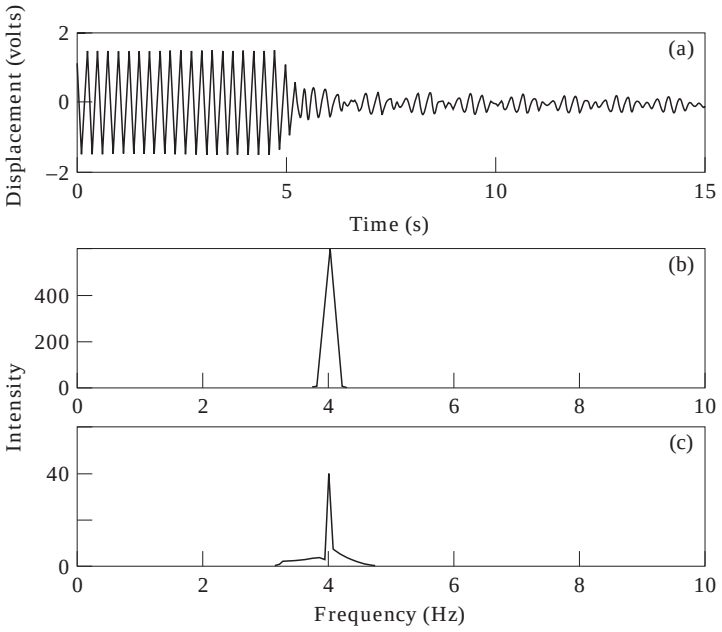

Figure 11. Experimental controlled response forced: $\omega_c = 24$ rad/s, $\zeta_c = 0{\cdot}09$; (a) plant response, (b) uncontrolled FFT, (c) controlled FFT.

too early, $\tau_d = 0{\cdot}74$, does not take advantage of the minimum yet to occur, as seen in Figure 10(a). However, if the disable is activated too late, $\tau_d = 1{\cdot}31$, as in Figure 10(c), then the remaining energy in the plant dissipates without the benefit of the control action. Finally, the optimum response $\tau_d = 0{\cdot}91$ is achieved when the disable is timed for exactly the first minimum.

For forced vibration, controller frequency ω_c is left at the optimal value of $\omega_c = 24$ rad/s. Since the controller is a continuous active vibration absorber, the initial condition of the controller is inconsequential to the over all response, hence it is set to zero. Moreover, the disable time is also insignificant as the controller is never disabled. Therefore, the only variable to have any significance to the plant response is the controller damping ζ_c. The method applied to activating the controller involves simulating the uncontrolled response until transients have dissipated, and then turning on the controller by introducing the coupling terms, and continuing the simulation from the final states of the uncontrolled response.

The beam is excited by a harmonic shaker as described earlier. The excitation frequency for this experiment is always the first natural frequency of the beam, 4·2 Hz. The beam transients are allowed to dissipate and the controller is only turned on when steady state is established. The plant responses each show the initial uncontrolled response, control activation, and controlled steady-state. The results for each case include FFT traces for the uncontrolled and controlled portions.

In Figure 11 the damping ratio is set to $\zeta_c = 0{\cdot}09$. It is observed that minimal phase shift occurs in the response; however, the amplitude decrease is reflected in the FFT. The controlled response is significantly improved over the uncontrolled case, and it is demonstrated by the breadth of the trace in the controlled FFT that the response is further improved. By measuring the magnitudes of the controlled and uncontrolled forced responses, there is an improved performance of over 80% over the uncontrolled response. For a detailed examination of the experimental system see reference [16].

7. CONCLUSIONS

This work employs the notion of using a secondary coupled co-ordinate for vibration absorption in an active control sense, which provides a significantly flexible enhancement to the classical passive vibration absorber, in that the same controller is used for free and forced vibration control. To this end, a linearized model is developed for a flexible cantilever beam with piezoceramic actuators. Upon coupling with the controller equations, this method results in a two-degree-of-freedom plant/controller set of governing equations which are solved. One advantage of this model is shown in that it is solved via analytical means resulting in a closed form solution, resulting in a computationally efficient method of analysis.

The responses examine a particular set of coupling terms which are determined experimentally, and yield the optimum energy exchange between co-ordinates. The LCC controller is simulated for a variety of conditions, by manipulating controller frequency, damping, initial condition and disable time.

In order to verify the model and analytical solution, a set of finite element simulations are also shown for the same physical parameters as the analytical model. The simulations are carried out for two inputs to the plant. The first case is for free vibration control, where an initial condition is imparted to the plant and the controller dissipates the oscillations. The second case is for forced vibration control, where a steady-state, harmonic, support excitation is simulated, and the controller operates continuously to dissipate energy. The results of the simulations confirm the efficacy of the controller strategy. For free vibration,

it is possible to tune a set of controller conditions such that the energy minimum in the plant can be achieved. Furthermore, the controller may be disabled in order to prevent energy from returning to the plant. When timed properly the controller reduced plant oscillations to zero. This occurred in a fraction of the time for a free response. For forced oscillations, the controller damping is manipulated in order to improve overall response. Experimental analysis demonstrated qualitative verification of the theoretical and finite element analysis solutions.

ACKNOWLEDGMENTS

The authors would like to express sincere thanks for the financial and material support of BM-HiTech Ltd. Collingwood, Ontario, Canada. This work was also supported by the Natural Sciences and Engineering Research Council of Canada.

REFERENCES

1. D. J. Inman 1994 *Engineering Vibrations*. Englewood Cliffs: Prentice-Hall; pp. 250–253.
2. S. G. Kelly 1973 *Fundamentals of Mechanical Vibrations*. New York: McGraw-Hill.
3. M. F. Golnaraghi 1991 *Dynamics and Control* **1**, 405–428. Regulation of flexible structures via nonlinear coupling.
4. A. Khajepour, M. F. Golnaraghi and K. A. Morris 1997 *Transactions of ASME, Journal of Vibration and Acoustics* **119,** 158–165. Application of center manifold theory to regulations of a flexible beam.
5. K. L. Tuer, A. P. Duquette and M. F. Golnaraghi 1993 *Journal of Sound and Vibration* **167**, 63–75. Vibration control of a flexible beam using a rotational internal resonance controller, part II: experiment.
6. K. L. Tuer, A. P. Duquette and M. F. Golnaraghi 1993 *Journal of Sound and Vibration* **167**, 41–62. Vibration control of a flexible beam using a rotational internal resonance controller, part I: theoretical development and analysis.
7. K. A. Morris and J. N. Juang 1994 *IEEE Transactions on Automatic Control* **39**, 1056–1063. Dissipative controller designs for second-order dynamic systems.
8. J. N. Juang and M. Phan 1992 *Journal of Guidance, Control, and Dynamics* **15**, 1192–1197. Robust controller designs for second order dynamic systems: a virtual approach.
9. S. S. Oueini and M. F. Golnaraghi 1996 *Journal of Sound and Vibration* **191**, 377–396. Experimental implementation of the internal resonance control strategy.
10. E. F. Crawley and E. H. Anderson 1989 In 30*th AIAA Structures, Structural Dynamics, and Materials Conference*, 2000–2010. Detailed models of piezoceramic actuation on beams.
11. D. J. Inman, H. H. Cudney and Y. Oshman 1990 In *Proceedings of AIAA/ASME/ASCE/AHS/ASC* 31*st Structures, Structural Dynamics and Materials Conference*, 2257–2264. Distributed parameter actuators for structural control.
12. B. Patnaik, G. R. Heppler and W. J. Wilson 1995 In 1995 *American Control Conference, Seattle WA*, 3840–3841. Structural property changes due to piezoelectric material bonding: a numerical example.
13. B. R. Patnaik 1994 *Master's thesis, University of Waterloo, Department of Systems Design Engineering*. Control of a tip-impacted arm and piezoelectric vibration suppression.
14. P. Salemi 1995 *Master's thesis, University of Waterloo, Department of Mechanical Engineering*. Numerical and experimental linear coupling control of free and forced vibration in a flexible structure.
15. R. W. Clough and J. Penzien 1975 *Dynamics of Structures*. New York: McGraw-Hill; pp. 154–155.
16. P. Salemi, M. F. Golnaraghi and G. R. Heppler 1995 In *Proceedings of the* 32*nd Annual Technical Meeting of the Society of Engineering Sciences*, 221–222. Experimental control of forced and unforced structural vibration using a linear coupling strategy.
17. L. Perko 1973 *Differential Equations and Dynamical Systems*. New York: Springer-Verlag.